Check for updates

IET Generation, Transmission & Distribution

Research Article

IET Journals
The Institution of Engineering and Technology

Generalised Cassie–Mayr electric arc furnace models

ISSN 1751-8687
Received on 22nd March 2016
Revised on 15th May 2016
Accepted on 1st June 2016
doi: 10.1049/iet-gtd.2016.0405
www.ietdl.org

Samaneh Golestani, Haidar Samet ✉

School of Electrical and Computer Engineering, Shiraz University, Shiraz, Iran
✉ *E-mail: samet@shirazu.ac.ir*

Abstract: Electric arc furnace (EAF) is one of the largest loads in the power systems. Unfortunately, it is highly non-linear and time varying which causes power quality problems such as harmonics and flicker. Therefore, having an accurate EAF model is necessary. Cassie model is one of the most utilised EAF models in the related fields. However, actual data from electrical system of Mobarakeh Steel Company in Isfahan/Iran show that this model is unable to take into account some important quantities such as the active power and harmonics. Hence, as the first step in this study, different Cassie–Mayr model variants (include the Cassie model) are investigated and the best variant is attained. A novel procedure using large number of recorded actual data is utilised for the models assessment. In the second step, two generalised types of the original Cassie–Mayr model are proposed. Both the generalised types are more accurate than the best-selected Cassie–Mayr variant. All the proposed models have time-varying parameters. Their time-varying nature is studied and by analysing the time series, the proper auto regressive moving average models are attained for every parameter.

Nomenclatures

R	arc resistance
τ	arc time constant
p_0	typical power loss of the arc
p_{0_1}, p_{0_2}	two different p_0 parameters used in the first generalised model
v_0	steady-state static arc voltage used in the Cassie model
i	arc current
v	arc voltage
α	parameter which leads to different Cassie–Mayr variants by taking different values
$\alpha1$, $\alpha2$	α parameters regarding the first generalised model
e_t	instantaneous residual error
e_i	mean error of instantaneous simulated current
e_v	mean error of instantaneous simulated voltage
e_{pi}	mean error of power using the simulated current
e_{pv}	mean error of power using the simulated voltage
e_{hij}	mean error of jth order current harmonic
e_{hvj}	mean error of jth order voltage harmonic
v_t	actual instantaneous value of voltage at tth sample
i_t	actual instantaneous value of current at tth sample
$\hat{v}_t$	simulated instantaneous value of voltage at tth sample
$\hat{i}_t$	simulated instantaneous value of current at tth sample
V_j	jth order of actual voltage harmonic
I_j	jth order of actual current harmonic
$\hat{V}_j$	jth order of simulated voltage harmonic
$\hat{I}_j$	jth order of simulated current harmonic
z_t	value of time series at time t
k	inverse value of the arc time constant. $k = 1/\tau$
m	inverse value of the arc time constant multiply by typical power loss of the arc. $m = 1/\tau p_0$ (when there is one α) or $m = 1/\tau p_{0_1}$ (related to $\alpha1$, when there are two α parameters)
n	inverse value of the arc time constant multiply by typical power loss of the arc. $n = 1/\tau p_{0_2}$ (related to $\alpha2$, when there are two α parameters)
Er	least mean square in a half cycle
t	index which shows the time sample number
UEI	unified error index
Ne_i	normalised mean error of the instantaneous simulated current
Ne_v	normalised mean error of the instantaneous simulated voltage
Ne_{pi}	normalised mean error of power using the simulated current
Ne_{pv}	normalised mean error of power using the simulated voltage
ANe_{hiJ}	average of normalised mean error of 2th, 3th, 4th, 5th, 6th and 7th order current harmonic
ANe_{hvJ}	average of normalised mean error of 2th, 3th, 4th, 5th, 6th and 7th order voltage harmonic
Ne_{hij}	normalised mean error of jth order current harmonic
Ne_{hvj}	normalised mean error of jth order voltage harmonic
Ne_v^g	normalised mean error of the instantaneous simulated voltage in the gth Cassie–Mayr model
e_v^g	mean error of the instantaneous simulated voltage in the gth Cassie–Mayr model
G	number of evaluated Cassie–Mayr models

1 Introduction

Electric arc furnace (EAF) is one of the largest single loads in power networks. It is widely used due to its productivity and low specific energy consumption [1]. However, it is a non-linear load [2], which generates a huge spectrum of harmonics. In addition, its time-varying nature causes unfavourable flicker [3, 4].

The above-mentioned reasons demonstrate the significance of having a comprehensive EAF model. A suitable EAF model should be able to extract the important quantities such as active power and harmonics correctly. In the EAF optimisation problems [5], it is important to use a model, which can extract the active power delivered to EAF exactly equal to real values in same conditions. Also accurate EAF modelling is essential for investigating its negative impacts on power system, evaluating the compensation techniques regarding to flicker and harmonics pollution [6–11], evaluating the arc stability [12] and evolution of protection techniques used in EAF plants [13, 14].

© The Institution of Engineering and Technology 2016

There are many attempts for EAF modelling. EAF models can be divided through different viewpoints [2]:

(i) *Linear or non-linear:* The function that relates EAF quantities such as voltage, current and resistance can be linear or non-linear. The simplest way of EAF modelling is to consider it as a variable resistance [15]. The linear model is successful in extracting the EAF fundamental frequency quantities such as active power. However, such a model is not applicable for harmonic studies. The hyperbolic function [16] and Cassie model [17] are two well-known non-linear models for EAF. Chook and Tan [18] state that bilinear model provides the best fitting for EAF in comparison with linear and direction-dependent models.

(ii) *Static or dynamic:* The model is dynamic, if its electrical quantities are dependent on their past values. In other words, if the model function consists of differential terms, it is dynamic. The Cassie model is a dynamic model. Another dynamic model, which consists of arc radius, current and voltage, is presented in [19]. The hyperbolic function model [16] is static.

(iii) *Time-varying or constant parameters:* EAF is a highly time-varying load, which causes voltage fluctuations that is known as flicker. The parameters of EAF model should be time varying to reflect its time-varying nature. There are several variation models introduced for EAF model parameters. In [16], a band-limited white noise is used to model the variation of arc length. In [3], auto regressive moving average (ARMA) models are used to model the variation of EAF reactive power. In [2], auto regressive (AR) models are used to model the variations of EAF model parameters. In [10], it is shown that ARMA models coefficients should be updated. Normalised least mean square [10], recursive least square [10] and genetic algorithm [20] are used to update ARMA models coefficients. The EAF reactive power forecasting is made by artificial neural network (ANN) in [21]. The non-linear characteristics of EAF reactive power variations are investigated in [22].

(iv) *Black box and white box models:* In black box models, EAF is modelled using ANN or similar techniques. Radial basis function networks are used in [23] to model EAF *v–i* characteristic. A method based on adaptive neuro-fuzzy inference systems for modelling EAFs is presented [24]. A neural network based method for modelling the non-linear EAF characteristic is described in [25]. An application of adaptive neuro-fuzzy networks is presented in [26]. However, the black-box models are hardly applicable in problems, which need an analytic model of EAF. Analytical model is applied in [18] to obtain a mathematical description, which can cover static and dynamic behaviours of EAF.

It is worth to mention that some studies have developed their modelling and simulation effort in the field of arc furnace with the aim of finite-element method. For example, [27] has used the advantages of finite-element method and added all the electromechanical coupling effects occurring in an EAF system in its modelling activity. A finite-element model of a DC arc furnace is investigated in [28] in order to predict the forces acting on the arc due to the magnetic field.

Among the large number of EAF models, Cassie model [17] is one of the most used models in the EAF studies. However, after large amounts of actual data from Mobarakeh Steel Company (MSC), Isfahan/Iran were gathered, we observed an unexpected result, which concluded that investigating previous models is unavoidable. It is found that even with selecting suitable parameters for Cassie model, still there are variances in some important quantities between experimental data and the model outputs.

The concentration of this article is on Cassie and various variants of Cassie–Mayr models [17]. To certify existing models, a large number of actual values of instantaneous currents and voltages at the secondary side of EAF transformers are utilised to calculate the models parameters. After determining the parameters for each half cycle, the model is ready to simulate.

The model is simulated by two methods. In the first method, the recorded actual EAF voltage is used as the input of the model and the current waveform is simulated. In the second method, the actual current is used as the input and the voltage is simulated. The simulated waveforms are compared with actual recorded waveforms. The comparison is made through calculations of average error indices related to instantaneous current and voltage and the average error corresponding to various current and voltage harmonic. In addition, the active power is calculated according to the simulated and actual waveforms and is used in the evaluation procedure. The active power is calculated in three cases: (i) using the actual voltage records and the simulated current, (ii) using the actual current records and the simulated voltage and(iii) using the actual recorded voltage and current. The mentioned evaluation procedure is done for a large number of Cassie–Mayr model variants to attain the most suitable variant regarding to harmonics and active power.

Further, to have more accurate models, the order of the original Cassie–Mayr model (α) is generalised in two types. At the first generalised type, the original Cassie–Mayr equation is extended to contain two values of α. In the second generalised type, the parameter α is assumed to be time varying and is updated every half cycle. The proposed extensions of Cassie–Mayr equation are evaluated using the mentioned procedure in the previous paragraph. It is found that both the generalised types are more accurate than the best-selected Cassie–Mayr variant. In order to develop the model in such a manner that does not complicate the calculation of the parameters, in both the proposed models, parameters are computable with linear least square method. Therefore, one of the important considerations in this article is to avoid non-linear formulation for calculating parameters of the proposed models, which makes it possible to decrease the error with less computational effort.

All the proposed EAF models in this paper have time-varying parameters, which change every half cycle. In the last section, they are considered as time series. ARMA models are applied and the most proper orders are attained for every parameter.

2 System under study

To calculate the EAF models parameters, actual input voltage and current waveform data were collected from eight EAFs installed in MSC, Isfahan, Iran. As it is shown in Fig. 1, the EAFs electric system is served by 400 kV transmission lines. Two transformers are used to step down the transmission voltage to 63 kV. Eight EAFs rated at 70 MW are connected through the flexible cables (between the EAF and EAF transformer), EAF transformers and the local feeders (between the main and EAF transformers) to the 63 kV bus.

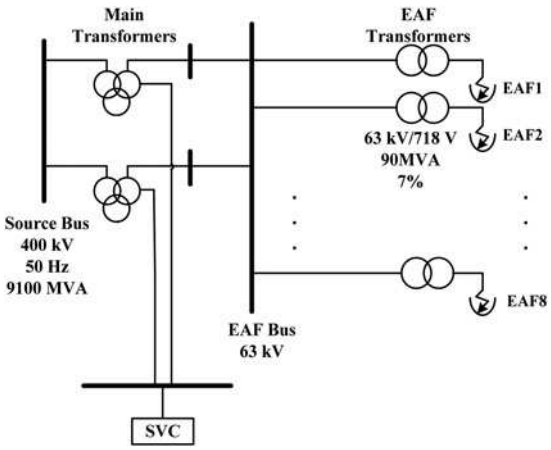

Fig. 1 *Structure of MSC*

© The Institution of Engineering and Technology 2016

17518695, 2016, 13, Downloaded from https://ietresearch.onlinelibrary.wiley.com/doi/10.1049/iet-gtd.2016.0405, Wiley Online Library on [06/05/2025]. See the Terms and Conditions (https://onlinelibrary.wiley.com/terms-and-conditions) on Wiley Online Library for rules of use; OA articles are governed by the applicable Creative Commons License

Data for the eight EAFs are collected within three months for scrapping, melting and refining stages of several melting processes. Three-phase instantaneous current and voltage are recorded at the secondary side of the EAF transformers. Hence, the flexible cable voltage drop, which is calculated by a simple equation using the recorded currents, should be deducted from the recorded voltage to attain the EAF voltage. The resistance and inductance of the flexible cable are equal to 0.33 mΩ and 7.18 μH. Every data record corresponds to the real-time furnace operation for 10 s. Since the sampling time is 128 μs, each data set consists of 78,125 samples. To sum up, the recorded data include 65 three-phase 10 s records and in total, there are 195 data sets.

3 Cassie–Mayr models

3.1 Cassie model

Cassie model is the most well-known EAF model which is structured as follows [17]

$$\frac{\mathrm{d}R}{\mathrm{d}t} = \frac{R}{\tau}\left(1 - \frac{v^2}{v_0^2}\right) \tag{1}$$

This formula has two coefficients; τ and v_0.

3.2 Mayr model

The structure of Mayr model is as follows

$$\frac{\mathrm{d}R}{\mathrm{d}t} = \frac{R}{\tau}\left(1 - \frac{vi}{p_0}\right) \tag{2}$$

3.3 Cassie–Mayr models

The main formula of Cassie–Mayr model is structured as

$$\frac{\mathrm{d}R}{\mathrm{d}t} = \frac{R}{\tau}\left(1 - \frac{vi}{p_0 R^{-\alpha}}\right) \tag{3}$$

Different values of α lead to different Cassie–Mayr variants. Cassie and Mayr are two special cases of the original Cassie–Mayr model where α is equal to one and zero, respectively. Lee *et al.* [17] proposes $0.5 < \alpha < 1$ as a reasonable range. Nonetheless, they specifically state: 'some experimental data shows the α values which is locally larger than one'.

4 Models evaluation procedure

The models evaluation procedure using the recorded actual data is presented in this section. The procedure consists of three steps as follows.

4.1 Model parameters calculation

The procedure here corresponds for a Cassie–Mayr model with order equal to α (3). For a known α, the model represented in (3) has two parameters τ and p_0. These parameters are calculated for every half cycle. There are some reasons for selecting the duration of half cycle in this study. The first reason is that the arc is turned on and turned off (if happens) once in each half cycle. Thus, this process is repeated in all half cycles [5, 29, 30]. The second reason is that the most common compensator for flicker mitigation in EAF plants is static VAr compensator (SVC) [7–10, 31, 32]. For this purpose, SVC injects the reactive power to the system with magnitude equal to the EAF reactive power but in the opposite direction. However due to the thyristor ignition and the calculation time for reactive power, SVC has a delay time about a half cycle for this application [3, 4, 8–10, 20–22, 31]. In other words, SVC needs one half cycle to react. Consequently, selecting shorter duration to update EAF parameters does not help to improve the SVC performance analysis. Also the effect of SVCs on flicker mitigation cannot be studied with EAF models that their update time of parameters is more than a half cycle. Hence, the parameters are time varying which are updated every 0.01 s. For every 10 s recorded data, model parameters are considered as a time series with length equal to 1000 samples.

Parameters in (3) are rewritten as follows

$$\frac{1}{\tau} = k, \quad \frac{1}{\tau p_0} = m \tag{4}$$

Thus

$$R' = R\left[k - m\frac{vi}{R^{-\alpha}}\right] \tag{5}$$

$$\frac{v'i - i'v}{i^2} = \frac{v}{i}\left[k - mv^{1+\alpha}i^{1-\alpha}\right] \tag{6}$$

Equation (6) is transformed to

$$ak + bm = d \tag{7}$$

where

$$\begin{cases} a = vi \\ b = -v^{2+\alpha}i^{2-\alpha} \\ d = v'i - i'v \end{cases} \tag{8}$$

To take advantage of least mean square method, error function must be minimised

$$\mathrm{Er} = \sum_{t=2}^{78} e_t^2 \tag{9}$$

The upper limit of (9) is equal to 78, which is the samples number in every half cycle ($78 = 0.01/0.000128$). The residual error (e_t) is calculated as follows

$$\begin{bmatrix} e_2 \\ . \\ . \\ . \\ e_t \end{bmatrix} = \begin{bmatrix} d_2 \\ d_3 \\ \vdots \\ d_t \end{bmatrix} - \begin{bmatrix} a_2 & b_2 \\ . & . \\ . & . \\ . & . \\ a_t & b_t \end{bmatrix} \begin{bmatrix} k \\ m \end{bmatrix} \overset{\text{yields}}{\rightarrow} E = D - A\boldsymbol{X} \tag{10}$$

Little consideration shows, matrix $\boldsymbol{X} = \begin{bmatrix} k \\ m \end{bmatrix}$ which minimise *Er* can be calculated from $\boldsymbol{X} = (A^{\mathrm{T}}A)^{-1}A^{\mathrm{T}}D$.

4.2 Model simulation

After calculation of model parameters for a considered α, the model should be simulated. Hence, the simulated data is compared with the actual data to evaluate the model. The simulation process is performed in two ways:

(i) In this method, the actual voltage data are utilised as the model input and the current is simulated as the model output. The simulation is performed every half cycle using the calculated parameters corresponding to that half cycle. At every half cycle the simulation starts from the zero crossing point of EAF current. At the start point, the simulated current value is considered to be equal to the actual value. Using (3), the current value at the latter

IET Gener. Transm. Distrib., 2016, Vol. 10, Iss. 13, pp. 3364–3373
© The Institution of Engineering and Technology 2016

17518695, 2016, 13, Downloaded from https://ietresearch.onlinelibrary.wiley.com/doi/10.1049/iet-gtd.2016.0405, Wiley Online Library on [06/05/2025]. See the Terms and Conditions (https://onlinelibrary.wiley.com/terms-and-conditions) on Wiley Online Library for rules of use; OA articles are governed by the applicable Creative Commons License

samples is calculated as the follows

$$i_{t+1} = i_t + \frac{\mathrm{d}t}{v_t}\left[\frac{\mathrm{d}v}{\mathrm{d}t}i_t - i_t\frac{v_t}{\tau}\left(1-\lambda(v_t^{1+\alpha}i_t^{1-\alpha})\right)\right] \tag{11}$$

(ii) This method is the same as the first method except, the actual current data is used as the model input to simulate the EAF voltage. At the start point the simulated voltage is considered equal to the actual value and voltage at the later moments is calculated as follows

$$v_{t+1} = v_t + \frac{\mathrm{d}t}{i_t}\left[\frac{\mathrm{d}i}{\mathrm{d}t}v_t + i_t\frac{v_t}{\tau}\left(1-\lambda(v_t^{1+\alpha}i_t^{1-\alpha})\right)\right] \tag{12}$$

4.3 Error indices

After the simulation of models, in the last stage of models evaluation the error indices are calculated. The error indices are as follows

$$e_i = \frac{1}{195\times 1000}\left(\sum_1^{195}\sum_1^{1000}\frac{\sum_{t=1}^{78}|i_t-\hat{i}_t|}{\sum_1^{78}|i_t|}\right) \tag{13}$$

$$e_v = \frac{1}{195\times 1000}\left(\sum_1^{195}\sum_1^{1000}\frac{\sum_{t=1}^{78}|v_t-\hat{v}_t|}{\sum_1^{78}|v_t|}\right) \tag{14}$$

$$e_{pi} = \frac{1}{195\times 1000}\left(\sum_1^{195}\sum_1^{1000}\frac{\left|\sum_{t=1}^{78}v_ti_t-\sum_{t=1}^{78}v_t\hat{i}_t\right|}{\left|\sum_{t=1}^{78}v_ti_t\right|}\right) \tag{15}$$

$$e_{pv} = \frac{1}{195\times 1000}\left(\sum_1^{195}\sum_1^{1000}\frac{\left|\sum_{t=1}^{78}v_ti_t-\sum_{t=1}^{78}\hat{v}_ti_t\right|}{\left|\sum_{t=1}^{78}v_ti_t\right|}\right) \tag{16}$$

$$e_{hij} = \frac{1}{195\times 1000}\left(\sum_1^{195}\sum_1^{1000}\frac{\left|I_j-\hat{I}_j\right|}{I_j}\right) \tag{17}$$

$$e_{hvj} = \frac{1}{195\times 1000}\left(\sum_1^{195}\sum_1^{1000}\frac{\left|V_j-\hat{V}_j\right|}{V_j}\right) \tag{18}$$

In the defined indices, 195, 1000 and 78 refer to the number of time series, number of half cycles in each time series and the number of samples in each half cycle.

In comparison to different EAF models, a model may have the minimum error value according to an index and some other models have the minimum values regarding to other indices. Hence, a unified error index (UEI) is defined which include all the defined error indices. The different error indices may have values, which are not in same range. Therefore, in the first step of calculating the UEI, for every error index the normalised value is calculated by dividing the error values to the average value related to all considered Cassie–Mayr models. For example, in case of considering G models in the comparison, the normalised e_v is as follows

$$Ne_v = \frac{e_v}{\left(\frac{1}{G}\sum e_v\right)} \tag{19}$$

UEI is defined as follows

$$\mathrm{UEI} = \frac{(Ne_i + Ne_v + Ne_{pi} + Ne_{pv} + ANe_{hiJ} + ANe_{hvJ})}{6} \tag{20}$$

where

$$ANe_{hiJ} = \frac{(Ne_{hi1}+Ne_{hi2}+Ne_{hi3}+Ne_{hi4}+Ne_{hi5}+Ne_{hi6}+Ne_{hi7})}{7}$$
$$ANe_{hvJ} = \frac{(Ne_{hv1}+Ne_{hv2}+Ne_{hv3}+Ne_{hv4}+Ne_{hv5}+Ne_{hv6}+Ne_{hv7})}{7} \tag{21}$$

5 Evaluation of Cassie–Mayr models

By varying the parameter α in (3) from 0 to 2.5 by steps equal to 0.1, 26 variants of Cassie–Mayr models are attained. All the 26 models are evaluated using all the recorded data with aid of the presented procedure Tables 1 and 2 show the defined error indices for all considered models. All error indices clearly decrease with increasing in the parameter α up to about 2. In other words, Cassie model ($\alpha = 1$) which is one of the most used models in the literature is not appropriate considering all error indices. On the other hand, the indices purposes high values of α equal to two. Fig. 2 shows the simulated and actual EAF voltage and current corresponding to one cycle of the recorded data for α equal to 0.5, 1 and 2 for one cycle. The figures show the improvement of the simulated signals by increasing α.

As it is shown in Table 1, the second minimum of UEI happens for $\alpha = 2$ and it is close the minimum value which is for $\alpha = 1.9$. As the simulations are simpler for $\alpha = 2$ than $\alpha = 1.9$, we suggest $\alpha = 2$ as the best variant of Cassie–Mayr model.

It is to be noted that the all parameters of the proposed model in this section are time varying and change at every half cycle except α which is equal to 2. In fact, it is observed that if the parameter τ in (3) be constant for all half cycles and equal to its mean value in the simulation stage, all error indices increase dramatically. Fig. 3 shows the variations of k and m parameters in (5) for 1 s based on $\alpha = 2$. Therefore, these parameters are assumed as time series and their time-varying nature will be discussed in the last section.

6 Generalised Cassie–Mayr models

The best variant of Cassie–Mayr models is attained in the previous section. Here, for further improvement in the model accuracy, two

Table 1 Error indices 1–4 and UEI for Cassie–Mayr models

α	e_i	e_v	e_{pi}	e_{pv}	UEI
0	0.6127	0.4612	0.5636	0.4121	3.3014
0.1	0.6044	0.4190	0.5583	0.3608	3.0642
0.2	0.5886	0.3731	0.5443	0.3034	2.7936
0.3	0.5696	0.3292	0.5268	0.2476	2.5272
0.4	0.5516	0.2922	0.5087	0.2012	2.2971
0.5	0.5419	0.2649	0.4984	0.1685	2.1824
0.6	0.5389	0.2676	0.4961	0.1696	2.1157
0.7	0.5359	0.2649	0.4956	0.1790	2.0921
0.8	0.5252	0.2497	0.4890	0.1663	2.0052
0.9	0.5028	0.2353	0.4721	0.1566	1.9169
1.0	0.4661	0.2237	0.4404	0.1501	1.8189
1.1	0.4165	0.2152	0.3938	0.1465	1.7025
1.2	0.3622	0.2090	0.3407	0.1448	1.5849
1.3	0.3147	0.2071	0.2917	0.1468	1.4912
1.4	0.2776	0.2107	0.2519	0.1550	1.4396
1.5	0.2516	0.1149	0.2232	0.0530	1.0977
1.6	0.2175	0.1000	0.1865	0.0397	0.8687
1.7	0.2004	0.0983	0.1669	0.0375	0.8218
1.8	0.1910	0.0990	0.1553	**0.0368**	0.8009
1.9	0.1865	**0.1008**	0.1488	0.0369	**0.7950**
2.0	**0.1839**	0.1037	0.1437	0.0376	**0.7964**
2.1	0.1845	0.1075	**0.1424**	0.0389	0.8074
2.2	0.1878	0.1118	0.1435	0.0408	0.8276
2.3	0.1931	0.1170	0.1469	0.0435	0.8545
2.4	0.2010	0.1232	0.1528	0.0474	0.8916
2.5	0.2305	0.1394	0.1809	0.0611	1.0727

Bold values illustrate the minimising trend of error to determine the best α

© The Institution of Engineering and Technology 2016

17518695, 2016, 13, Downloaded from https://ietresearch.onlinelibrary.wiley.com/doi/10.1049/iet-gtd.2016.0405, Wiley Online Library on [06/05/2025]. See the Terms and Conditions (https://onlinelibrary.wiley.com/terms-and-conditions) on Wiley Online Library for rules of use; OA articles are governed by the applicable Creative Commons License

Table 2 Error indices 5 and 6 for Cassie–Mayr models

α	e_{hi1}	e_{hi2}	e_{hi3}	e_{hi4}	e_{hi5}	e_{hi6}	e_{hi7}	e_{hv1}	e_{hv2}	e_{hv3}	e_{hv4}	e_{hv5}	e_{hv6}	e_{hv7}
0	0.62	0.97	1.07	1.07	1.09	1.08	1.07	0.57	0.62	0.57	0.53	0.52	0.52	0.52
0.1	0.62	0.93	1.02	1.02	1.04	1.03	1.03	0.51	0.59	0.53	0.49	0.48	0.47	0.47
0.2	0.61	0.87	0.95	0.95	0.97	0.97	0.96	0.45	0.55	0.50	0.45	0.43	0.42	0.42
0.3	0.59	0.80	0.87	0.87	0.89	0.89	0.89	0.39	0.51	0.47	0.42	0.39	0.38	0.37
0.4	0.56	0.72	0.79	0.80	0.81	0.81	0.82	0.34	0.47	0.44	0.39	0.36	0.35	0.34
0.5	0.55	0.67	0.73	0.74	0.75	0.76	0.76	0.34	0.48	0.46	0.42	0.39	0.37	0.36
0.6	0.55	0.64	0.69	0.70	0.71	0.72	0.73	0.27	0.42	0.40	0.38	0.34	0.32	0.31
0.7	0.55	0.62	0.67	0.68	0.69	0.70	0.71	0.22	0.38	0.37	0.35	0.33	0.31	0.29
0.8	0.55	0.61	0.65	0.66	0.68	0.69	0.69	0.19	0.34	0.34	0.34	0.32	0.30	0.29
0.9	0.54	0.59	0.63	0.64	0.66	0.67	0.68	0.16	0.31	0.32	0.33	0.31	0.30	0.28
1.0	0.48	0.54	0.58	0.59	0.61	0.62	0.63	0.15	0.28	0.30	0.31	0.31	0.29	0.28
1.1	0.40	0.47	0.51	0.52	0.53	0.55	0.55	0.14	0.26	0.29	0.30	0.30	0.29	0.28
1.2	0.32	0.42	0.45	0.46	0.47	0.48	0.49	0.13	0.24	0.27	0.29	0.29	0.28	0.27
1.3	0.27	0.39	0.42	0.42	0.43	0.44	0.44	0.13	0.23	0.26	0.28	0.28	0.28	0.27
1.4	0.24	0.37	0.40	0.40	0.41	0.41	0.41	0.13	0.22	0.25	0.27	0.28	0.27	0.26
1.5	0.22	0.35	0.38	0.38	0.39	0.39	0.40	0.17	0.26	0.30	0.32	0.32	0.31	0.30
1.6	0.19	0.34	**0.37**	0.37	0.37	**0.37**	0.37	**0.09**	**0.18**	0.22	0.23	0.23	0.22	0.22
1.7	0.17	**0.33**	**0.37**	**0.36**	**0.36**	**0.37**	**0.36**	**0.09**	**0.18**	**0.21**	0.23	0.22	0.22	0.21
1.8	0.17	**0.33**	**0.37**	0.37	0.37	**0.37**	**0.36**	**0.09**	**0.18**	**0.21**	**0.22**	0.22	**0.21**	**0.20**
1.9	**0.16**	0.34	0.38	0.37	0.37	**0.37**	0.37	**0.09**	0.19	0.22	**0.22**	0.22	**0.21**	**0.20**
2.0	**0.16**	0.34	0.39	0.38	0.38	0.38	0.38	0.10	0.19	0.22	**0.22**	**0.21**	**0.21**	**0.20**
2.1	0.16	0.35	0.40	0.39	0.39	0.39	0.39	0.10	0.20	0.23	0.23	0.22	**0.21**	**0.20**
2.2	0.17	0.37	0.41	0.41	0.41	0.41	0.40	0.11	0.21	0.23	0.23	0.22	**0.21**	**0.20**
2.3	0.17	0.38	0.43	0.42	0.42	0.42	0.42	0.11	0.22	0.24	0.23	0.22	**0.21**	**0.20**
2.4	0.18	0.39	0.44	0.44	0.44	0.44	0.44	0.12	0.23	0.24	0.23	0.22	**0.21**	**0.20**
2.5	0.19	0.42	0.47	0.47	0.47	0.47	0.47	0.19	0.30	0.31	0.30	0.29	0.28	0.27

Bold values illustrate the minimising trend of error to determine the best α

generalised types of Cassie–Mayr model are proposed. The two types are based on this fact that there is no exact value for α in (3).

6.1 Utilising two α parameters

In the first generalised model, two values of α are utilised in the original Cassie–Mayr equation as follows

$$\frac{\mathrm{d}R}{\mathrm{d}t} = \frac{R}{\tau}\left(1 - \frac{vi}{p_{0_1}R^{-\alpha 1}} - \frac{vi}{p_{0_2}R^{-\alpha 2}}\right) \tag{22}$$

Parameters in this formula are rewritten as follows

$$\frac{1}{\tau} = k, \quad \frac{1}{\tau p_{0_1}} = m, \quad \frac{1}{\tau p_{0_2}} = n \tag{23}$$

Thus

$$R' = R\left[k - m\frac{vi}{R^{-\alpha 1}} - n\frac{vi}{R^{-\alpha 2}}\right] \tag{24}$$

$$\frac{v'i - i'v}{i^2} = \frac{v}{i}\left[k - mv^{1+\alpha 1}i^{1-\alpha 1} - nv^{1+\alpha 2}i^{1-\alpha 2}\right] \tag{25}$$

Equation (22) is transformed to

$$ak + bm + cn = d \tag{26}$$

where

$$\begin{cases} a = vi \\ b = -v^{2+\alpha 1}i^{2-\alpha 1} \\ c = -v^{2+\alpha 2}i^{2-\alpha 2} \\ d = v'i - i'v \end{cases} \tag{27}$$

Same to the procedure for the original Cassie–Mayr model, the error function (6) must be minimised. The residual error e_n in (6) can be calculated as follows for the generalised model

$$\begin{bmatrix} e_2 \\ e_3 \\ \vdots \\ e_t \end{bmatrix} = \begin{bmatrix} d_2 \\ d_3 \\ \vdots \\ d_t \end{bmatrix} - \begin{bmatrix} a_2 & b_2 & c_2 \\ a_3 & b_3 & c_3 \\ \vdots & \vdots & \vdots \\ a_t & b_t & c_t \end{bmatrix} \begin{bmatrix} k \\ m \\ n \end{bmatrix} \overset{\text{yields}}{\rightarrow} E = D - A\boldsymbol{X} \tag{28}$$

Little consideration shows, vector $\boldsymbol{X} = \begin{bmatrix} k \\ m \\ n \end{bmatrix}$ which minimises Er can be calculated from $\boldsymbol{X} = (A^{\mathrm{T}}A)^{-1}A^{\mathrm{T}}D$.

After calculation of model parameters for a considered pair (α_1, α_2), the model should be simulated. The simulated data are compared with the actual ones. Equations (29) and (30) are derived as same as (11) and (12)

$$i_{t+1} = \frac{\mathrm{d}t}{v_t}\left[v'i_t - \left[kv_ti_t - mv_t^{2+\alpha_1}i_t^{2-\alpha_1} - nv_t^{2+\alpha_2}i_t^{2-\alpha_2}\right]\right] + i_t \tag{29}$$

$$v_{t+1} = \frac{\mathrm{d}t}{i_t}\left[-i'v_t + \left[kv_ti_t - mv_t^{2+\alpha_1}i_t^{2-\alpha_1} - nv_t^{2+\alpha_2}i_t^{2-\alpha_2}\right]\right] + v_t \tag{30}$$

By varying α_1 and α_2 in (22) from 0 to 2.5 by steps equal to 0.1, 312 variants of the first type of generalised Cassie–Mayr models are attained. Table 3 shows the UEI for all models. The results show that model ($\alpha_1 = 2.1$, $\alpha_2 = 0.1$) has the minimum UEI. However, the model ($\alpha_1 = 2$, $\alpha_2 = 0$) is selected here as the most appropriate model because it needs less computational burden and its UEI is close to the minimum value.

Table 4 shows the error indices related to the best variants of the original Cassie–Mayr model, the first type generalised model and the second type. Comparing the original model with the first generalised type ($\alpha_1 = 2$, $\alpha_2 = 0$), reveals a considerable reduction in all error indices. Fig. 4 shows the simulated and corresponding actual EAF voltage and current for the generalised model with ($\alpha_1 = 2$, $\alpha_2 = 0$) and for the original Cassie–Mayr model with ($\alpha = 2$). The improvement in the simulated waveforms in the case of the

© The Institution of Engineering and Technology 2016

17518695, 2016, 13, Downloaded from https://ietresearch.onlinelibrary.wiley.com/doi/10.1049/iet-gtd.2016.0405, Wiley Online Library on [06/05/2025]. See the Terms and Conditions (https://onlinelibrary.wiley.com/terms-and-conditions) on Wiley Online Library for rules of use; OA articles are governed by the applicable Creative Commons License

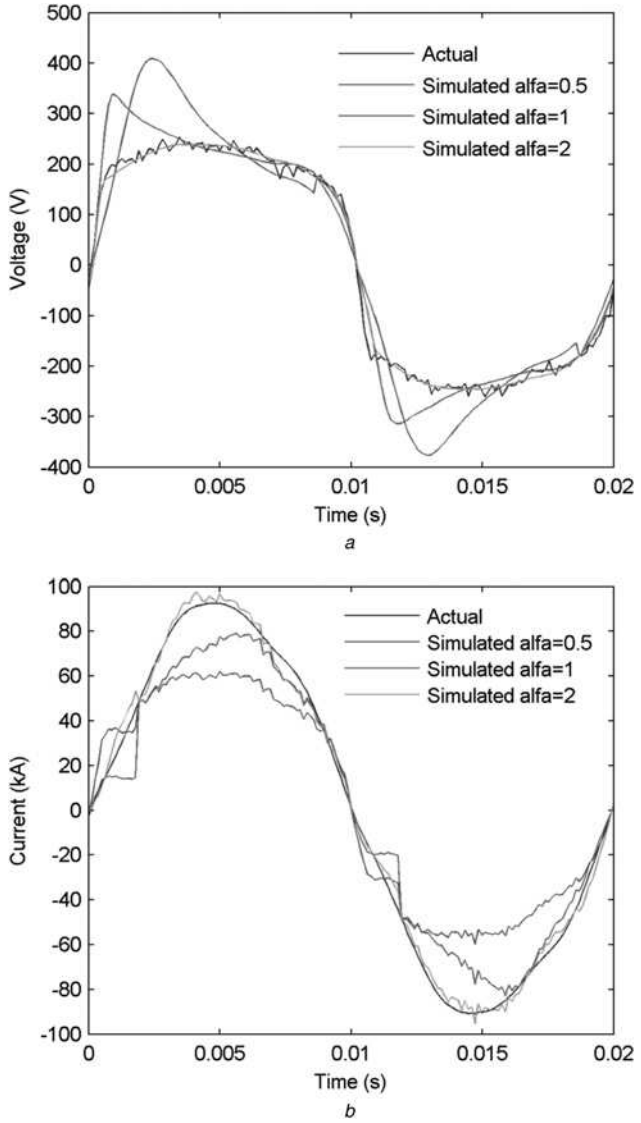

Fig. 2 *Actual and simulated waveforms for different Cassie–Mayr models*
a Voltage
b Current

generalised model is evidence in the figures. In addition, Fig. 5 shows the variations of model parameters for ($\alpha_1 = 2$, $\alpha_2 = 0$) over 1 s.

6.2 Time-varying α parameter

In all previous sections, the value of α parameter is kept constant over the time. However, all other models parameters were time varying. As the second generalised type of Cassie–Mayr, α in (3) is considered to change every half cycle. To attain the best α for each half cycle, models with α between 0 and 2.5 with steps equal to 0.1 are checked for the corresponding half cycle. The model, which minimises $ne_i + ne_v$ is chosen as the best model for that half cycle. Fig. 6 shows the variations of α over 1 s, which can be considered as a time series. The error indices values in Table 4 indicate that the Cassie–Mayr model with time varying α has the lowest error indices compared with the best variants of the two other models.

7 Time series modelling of EAF models parameters

In the previous sections, calculation of EAF model parameters is made at every half cycle. In fact, it is found that considering a parameter (such as τ) to be constant over all cycles, scarifies the model accuracy. This fact is evident because of the stochastic and time-varying nature of EAF. Hence, for a 10 s data record, every parameter can be considered as a time series with length equal to 1000 (= 10/0.01). The following time-varying parameters are studied in this section:

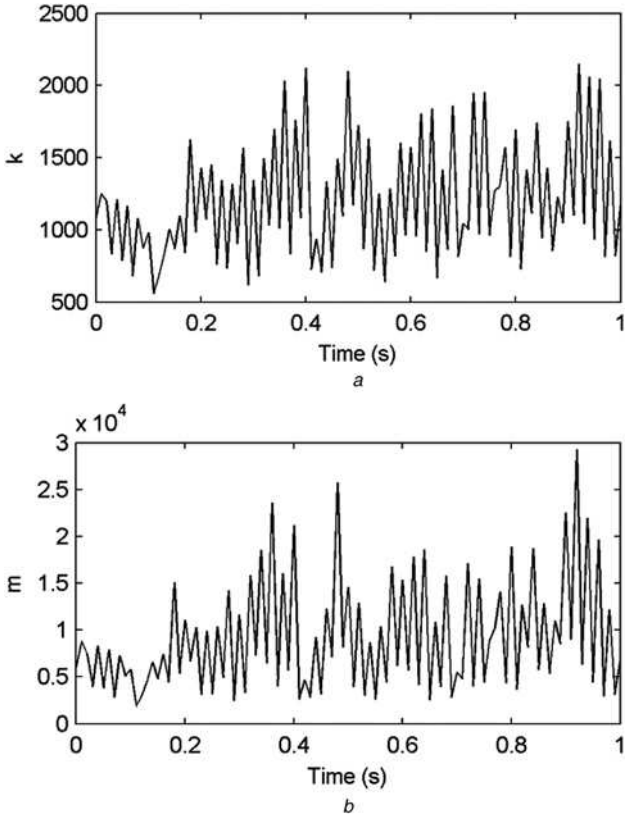

Fig. 3 *Variations of Cassie–Mayr model parameters with $\alpha = 2$*
a Parameter *n*
b Parameter *m*

(i) Parameters k and m in the original Cassie–Mayr model with $\alpha = 2$.
(ii) Parameters k, m and n in first type of generalised Cassie–Mayr model with $\alpha_1 = 2$ and $\alpha_2 = 0$.
(iii) Parameters α and k and m in the second type of generalised Cassie–Mayr model.

To begin, auto correlation function (ACF) is utilised to show the correlation between the mentioned parameters in consecutive half cycles. To consider all the recorded data, the ACF regarding to every recorded data is calculated and then its average considering all records (195 records) is calculated. The average ACF for some of the mentioned parameters is presented in Fig. 7. The ACF values for lags equal to or larger than one are somewhat large. This fact shows that the time-varying nature of model parameters is not as a white noise and there is dependability between the parameters in the consecutive half cycles. In fact, the parameters are predictable for the next half cycles.

In the second step, ARMA models are utilised for time series modelling. An ARMA model of order (p, q) which is denoted as ARMA(p, q) is given by

$$z_t = \varphi_1 z_{n-1} + \ldots + \varphi_p z_{n-p} + a_n - \theta_1 a_{n-1} - \ldots - \theta_q a_{n-q} \quad (31)$$

z_t is assumed to be a zero average time series. If z_t has non-zero average, it can be replaced with $z_t - \mu$ where μ is the mean of z_t. If in ARMA(p,q) process $q = 0$, it is called AR(p) process and if $p = 0$ it is called MA(q) process.

© The Institution of Engineering and Technology 2016

17518695, 2016, 13, Downloaded from https://ietresearch.onlinelibrary.wiley.com/doi/10.1049/iet-gtd.2016.0405, Wiley Online Library on [06/05/2025]. See the Terms and Conditions (https://onlinelibrary.wiley.com/terms-and-conditions) on Wiley Online Library for rules of use; OA articles are governed by the applicable Creative Commons License

Table 3 UEI for the first type of generalised Cassie–Mayr models

	0.1	0.2	0.3	0.4	0.5	0.6	0.7	0.8	0.9	1	1.1	1.2	1.3	1.4	1.5	1.6	1.7	1.8	1.9	2	2.1	2.2	2.3	2.4	2.5
0	1.119	1.115	1.132	1.192	1.235	1.194	1.156	1.125	1.102	1.090	1.089	1.102	1.134	1.161	1.011	0.752	0.721	0.704	0.694	**0.685**	0.684	0.688	0.698	0.713	0.866
0.1		1.127	1.157	1.214	1.209	1.174	1.140	1.112	1.095	1.090	1.084	1.101	1.133	1.162	1.017	0.754	0.723	0.705	0.695	0.685	**0.683**	0.687	0.695	0.709	0.858
0.2			1.191	1.212	1.186	1.153	1.125	1.102	1.087	1.081	1.085	1.104	1.140	1.166	1.018	0.756	0.725	0.708	0.697	0.687	0.685	0.688	0.694	0.708	0.853
0.3				1.193	1.161	1.135	1.111	1.094	1.082	1.082	1.087	1.110	1.150	1.179	1.017	0.757	0.728	0.711	0.699	0.689	0.687	0.689	0.695	0.707	0.850
0.4					1.140	1.118	1.100	1.087	1.080	1.082	1.092	1.123	1.170	1.199	1.007	0.759	0.731	0.713	0.702	0.692	0.690	0.690	0.696	0.708	0.855
0.5						1.104	1.093	1.083	1.081	1.085	1.103	1.149	1.201	1.225	0.976	0.761	0.734	0.716	0.706	0.695	0.692	0.692	0.698	0.710	0.945
0.6							1.086	1.083	1.084	1.094	1.126	1.200	1.225	1.256	0.935	0.763	0.736	0.720	0.710	0.701	0.697	0.696	0.702	0.714	1.030
0.7								1.085	1.092	1.112	1.184	1.235	1.233	1.251	0.944	0.775	0.744	0.729	0.720	0.709	0.707	0.708	0.718	0.746	1.132
0.8									1.108	1.167	1.246	1.236	1.249	1.155	0.948	0.797	0.761	0.744	0.734	0.724	0.724	0.730	0.747	0.794	1.144
0.9										1.250	1.242	1.243	1.218	1.117	0.948	0.823	0.785	0.767	0.757	0.748	0.753	0.763	0.785	0.842	1.142
1											1.243	1.235	1.154	1.079	0.949	0.848	0.813	0.796	0.787	0.781	0.786	0.798	0.826	0.888	1.148
1.1												1.174	1.114	1.034	0.943	0.871	0.841	0.828	0.821	0.817	0.825	0.841	0.873	0.936	1.160
1.2													1.062	1.003	0.936	0.890	0.870	0.861	0.858	0.858	0.870	0.887	0.916	0.976	1.179
1.3														0.985	0.932	0.911	0.901	0.899	0.899	0.901	0.910	0.925	0.952	1.001	1.198
1.4															0.935	0.929	0.929	0.933	0.936	0.939	0.946	0.956	0.974	1.015	1.222
1.5																0.947	0.953	0.956	0.961	0.962	0.964	0.962	0.955	0.931	1.026
1.6																	0.970	0.976	0.978	0.973	0.965	0.939	0.914	0.878	0.939
1.7																		0.985	0.983	0.964	0.939	0.912	0.887	0.861	0.946
1.8																			0.970	0.944	0.917	0.895	0.874	0.890	0.960
1.9																				0.917	0.902	0.886	0.896	0.932	0.962
2																					0.892	0.902	0.929	0.947	0.926
2.1																						0.928	0.944	0.936	0.876
2.2																							0.935	0.891	0.855
2.3																								0.857	0.855
2.4																									0.867

Bold values illustrate the minimising trend of error to determine the best α

© The Institution of Engineering and Technology 2016

17518695, 2016, 13, Downloaded from https://ietresearch.onlinelibrary.wiley.com/doi/10.1049/iet-gtd.2016.0405, Wiley Online Library on [06/05/2025]. See the Terms and Conditions (https://onlinelibrary.wiley.com/terms-and-conditions) on Wiley Online Library for rules of use; OA articles are governed by the applicable Creative Commons License

Table 4 UEI for the first type of generalised Cassie–Mayr models

	Original $\alpha = 2$	Two α parameters $\alpha_1 = 2$ and $\alpha_2 = 0$	Time varying α
e_i	0.1839	0.1499	0.0845
e_v	0.1037	0.0868	0.0627
e_{pi}	0.1437	0.1141	0.0485
e_{pv}	0.0376	0.0334	0.0145
e_{hi1}	0.1628	0.1284	0.0600
e_{hi2}	0.3445	0.2542	0.1552
e_{hi3}	0.3877	0.3161	0.2099
e_{hi4}	0.3809	0.3157	0.2117
e_{hi5}	0.3819	0.3137	0.2107
e_{hi6}	0.3823	0.3101	0.2158
e_{hi7}	0.3781	0.3058	0.2136
e_{hv1}	0.0965	0.0786	0.0524
e_{hv2}	0.1914	0.1448	0.1183
e_{hv3}	0.2200	0.1865	0.1538
e_{hv4}	0.2237	0.2089	0.1736
e_{hv5}	0.2150	0.2080	0.1749
e_{hv6}	0.2056	0.2027	0.1714
e_{hv7}	0.1965	0.1948	0.1630

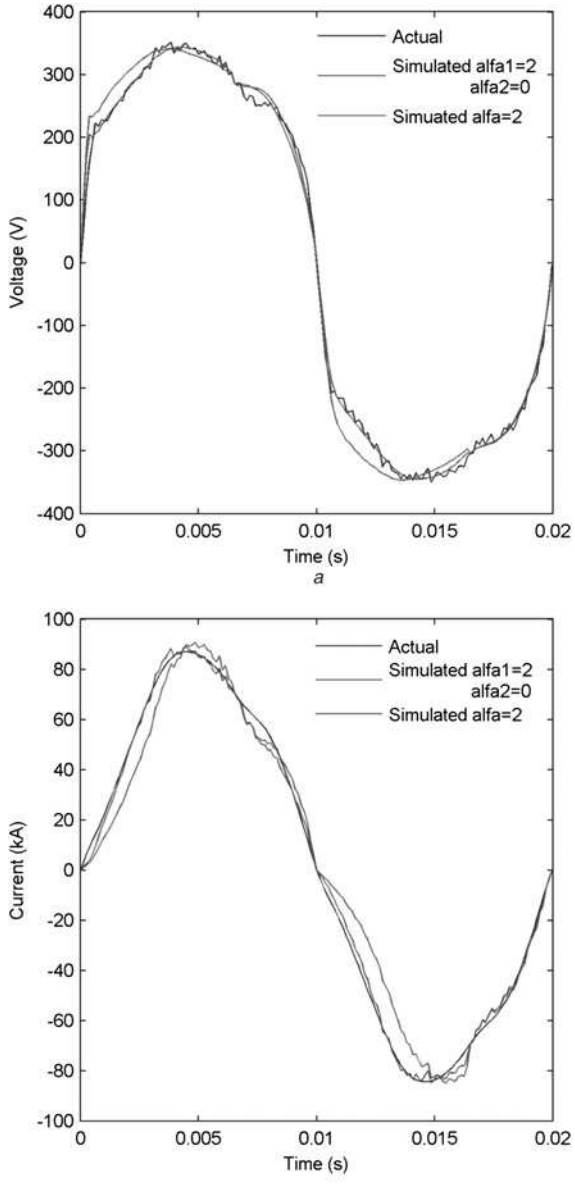

Fig. 4 *Actual and simulated current for the best Cassie–Mayr model and the best generalised model*

a Voltage
b Current

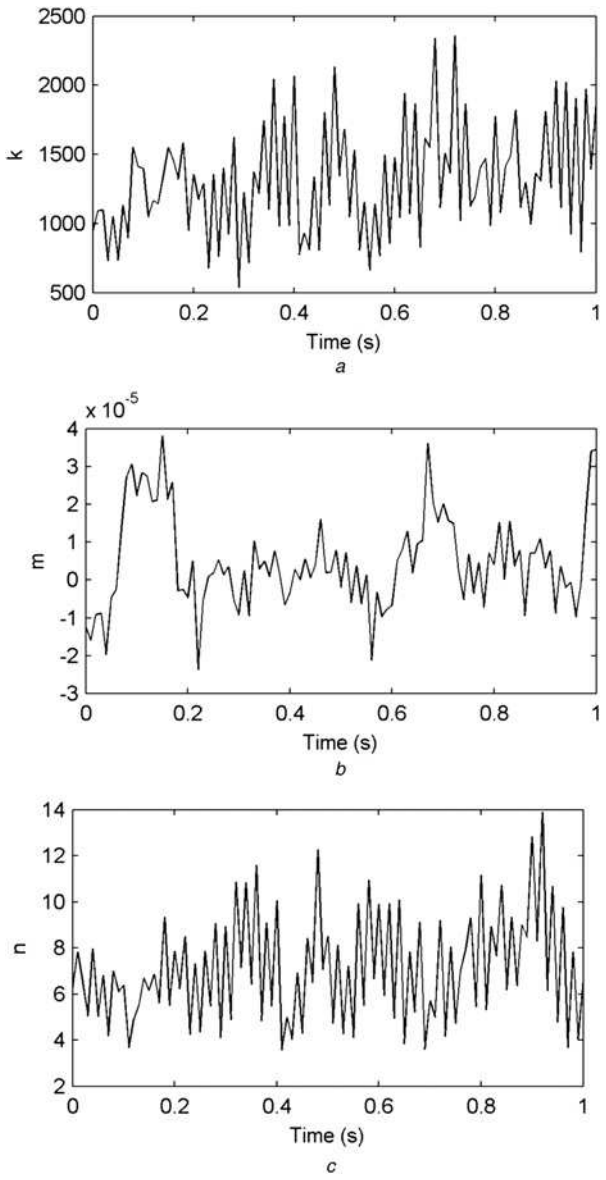

Fig. 5 *Variations of parameters in (24) for ($\alpha_1 = 2$, $\alpha_2 = 0$)*

a Parameter *k*
b Parameter *m*
c Parameter *n*

Two model adequacy-checking tests are used to attain the best order ARMA models for every mentioned parameter. The utilised tests are Akaike information criterion (AIC) and Schwarz criterion

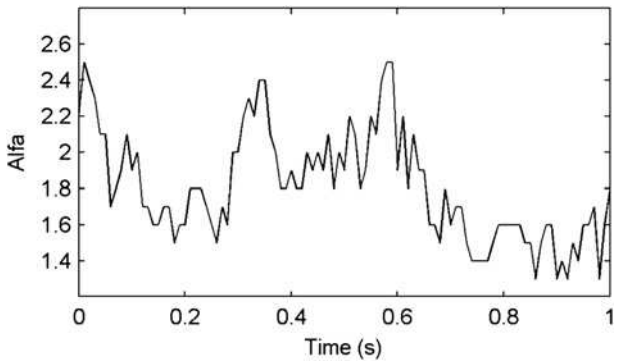

Fig. 6 *Variations of α parameter in (3) for the second generalised model*

© The Institution of Engineering and Technology 2016

17518695, 2016, 13, Downloaded from https://ietresearch.onlinelibrary.wiley.com/doi/10.1049/iet-gtd.2016.0405, Wiley Online Library on [06/05/2025]. See the Terms and Conditions (https://onlinelibrary.wiley.com/terms-and-conditions) on Wiley Online Library for rules of use; OA articles are governed by the applicable Creative Commons License

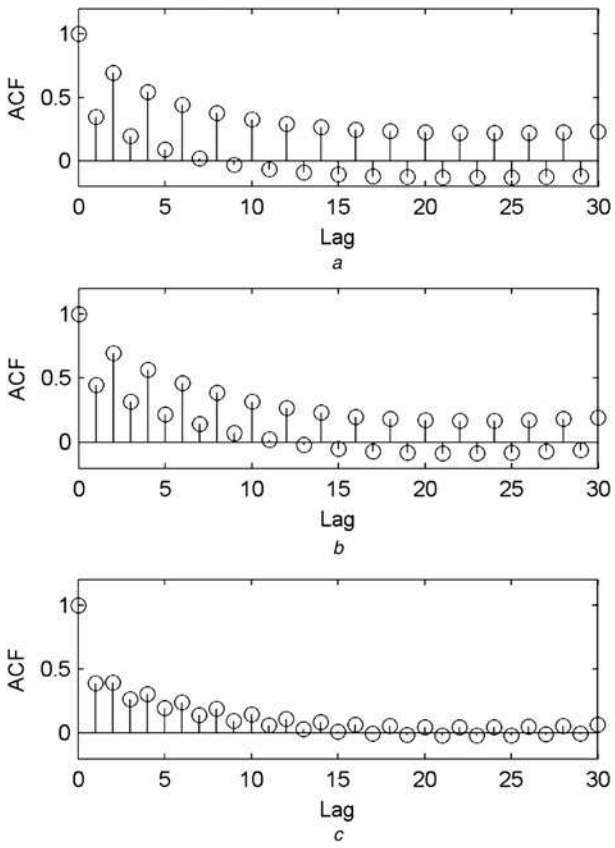

Fig. 7 *Average ACF*

a For parameter k in the original Cassie–Mayr model with $\alpha = 2$
b For parameter k in first type of generalised Cassie–Mayr model with $\alpha_1 = 2$ and $\alpha_2 = 0$
c For parameter α in second type of generalised Cassie–Mayr model

Table 5 ARMA orders based on AIC and SC tests

EAF model	Parameter	AIC test	SC test
original Cassie–Mayr	k	AR(9), ARMA (5,2), ARMA (2,5)	ARMA(4,1), ARMA(3,2)
	m	AR(9), ARMA(5,2)	ARMA(4,1)
first type generalised Cassie–Mayr	k	AR(9), ARMA (5,2), ARMA (2,5)	ARMA(3,1), ARMA(4,2)
	m	AR(9), ARMA (5,2), ARMA (2,5)	ARMA(3,1), ARMA(4,2)
	n	AR(9), ARMA (5,2), ARMA (2,5)	ARMA(3,1), ARMA(4,2)
second type generalised Cassie–Mayr	α	AR(9), ARMA(2,2)	AR(4), ARMA (2,2)
	k	AR(9), ARMA (2,2), ARMA (2,5)	ARMA(2,2)
	m	AR(9)	AR(4), ARMA (2,2)

(SC) which are applied to all the 195 time series for every model parameter. Table 5 presents the selected ARMA orders for the EAF models parameters.

8 Conclusions

Cassie–Mayr models are investigated for EAF modelling. A novel assessment procedure using a large number of practical records is utilised. It is shown that Cassie model, the most used EAF model, is not accurate. Through comprehensive analysis, this paper proposes three models for EAF. The first model is attained by evaluating the original Cassie–Mayr model with different α parameter. The two other proposed models are attained by two generalised types of the original Cassie–Mayr model. Therefore, the proposed three models are as follows:

(i) By investigating different variants of Cassie–Mayr model, it is found that the variant with $\alpha = 2$ is the most proper model for EAF. However, the two other parameters that exist in this model should be time varying and be updated every half cycle.
(ii) In the first generalised type of Cassie–Mayr model, the original Cassie–Mayr equation is extended to contain two values of α. By evaluating 312 variants of this extended model, the most proper model is attained ($\alpha_1 = 2$, $\alpha_2 = 0$).
(iii) In the second generalised type, the parameter α is updated every half cycle besides other parameters in the original Cassie–Mayr model. The second generalised type is the most accurate followed by the first generalised type and then the original Cassie–Mayr model with $\alpha = 2$.

In all the proposed EAF models, parameters are time varying and change every half cycle. Hence, they are considered as time series. It is found that there is a considerable correlation between the parameters values at past half cycles with the present half cycle and hence they are predictable. ARMA models are applied and the most proper orders are attained for every parameter.

9 References

1 Arens, M., Worrell, E., Schleich, J.: 'Energy intensity development of the German iron and steel industry between 1991 and 2007', *Energy*, 2012, **45**, (1), pp. 786–797
2 Samet, H., Farjah, E., Sharifi, Z.: 'A dynamic, nonlinear and time-varying model for electric arc furnace', *Int. Trans. Electr. Energy Syst.*, 2015, **25**, (10), pp. 2165–2180
3 Samet, H., Golshan, M.E.H.: 'Employing stochastic models for prediction of arc furnace reactive power to improve compensator performance', *IET Gener. Transm. Distrib.*, 2008, **2**, (4), pp. 505–515
4 Samet, H., Mojallal, A.: 'Enhancement of electric arc furnace reactive power compensation using Grey-Markov prediction method', *IET Gener. Transm. Distrib.*, 2014, **8**, (9), pp. 1626–1636
5 Samet, H., Ghanbari, T., Ghaisari, J.: 'Maximum performance of electric arc furnace by optimal setting of the series reactor and transformer taps using a nonlinear model', *IEEE Trans. Power Deliv.*, 2015, **30**, (2), pp. 764–772
6 Bhonsle, D.C., Kelkar, R.B.: 'Design and analysis of composite filter for power quality improvement of electric arc furnace'. Third Int. Conf. on Electric Power and Energy Conversion Systems (EPECS), 2013, pp. 1–10
7 Dionise, T.: 'Assessing the performance of a static VAr compensator for an electric arc furnace', *IEEE Trans. Ind. Appl.*, 2013, **5**, (3), pp. 1619–1629
8 Samet, H., Parniani, M.: 'Predictive method for improving SVC speed in electric arc furnace compensation', *IEEE Trans. Power Deliv.*, 2007, **22**, (1), pp. 732–734
9 Samet, H., Mojallal, A., Ghanbari, T.: 'Employing grey system model for prediction of electric arc furnace reactive power to improve compensator performance', *Prz. Elektrotech.*, 2013, **89**, (12), pp. 110–115
10 Golshan, M.E.H., Samet, H.: 'Updating stochastic model coefficients for prediction of arc furnace reactive power', *Electr. Power Syst. Res.* , 2009, **79**, (7), pp. 1114–1120
11 Hsu, Y.J., Chen, K.H., Huang, P.Y., *et al.*: 'Electric arc furnace voltage flicker analysis and prediction', *IEEE Trans. Instrum. Meas.*, 2011, **60**, (10), pp. 3360–3368
12 Kim, S.H., Jeong, J.J., Kim, K., *et al.*: 'Arc stability index using phase electrical power in AC electric arc furnace'. 13th Int. Conf. on Control, Automation and Systems, Gwangju, 2013, pp. 1725–1728
13 Kojovic, L.A., Bishop, M.T., Sharma, D.: 'Innovative differential protection of power transformers using low-energy current sensors', *IEEE Trans. Ind. Appl.*, 2013, **49**, (5), pp. 1971–1978
14 Dehghan, F., Samet, H.: 'Fault detection in the secondary side of electric arc furnace transformer using the primary side data', *Int. Trans. Electr. Energy Syst.*, 2014, **24**, (10), pp. 1419–1433
15 Manchur, G., Erven, C.C.: 'Development of a model for predicting flicker from electric arc furnaces', *IEEE Trans. Power Deliv.*, 1992, **7**, (1), pp. 416–426
16 Cavallini, A., Montanari, G.C., Pitti, L., *et al.*: 'ATP simulation for arc-furnace flicker investigation', *Eur. Trans. Electr. Power*, 2007, **5**, (3), pp. 165–172
17 Lee, Y.J., Suh, Y., Nordborg, H., *et al.*: 'Arc stability criteria in AC arc furnace and optimal converter topologies'. Proc. of 22 IEEE Applied Power Electronics Conf. (APEC), 2007, pp. 1280–1286
18 Chook, K.C., Tan, A.H.: 'Identification of an electric resistance furnace', *IEEE Trans. Instrum. Meas.*, 2007, **56**, (6), pp. 2262–2270
19 Acha, E., Semlyen, A., Rajakovic, N.: 'A harmonic domain computational package for nonlinear problems and its applications to electric arcs', *IEEE Trans. Power Deliv.*, 1990, **5**, (3), pp. 1390–1397
20 Golshan, M.E.H., Samet, H.: 'Updating stochastic models of arc furnace reactive power by genetic algorithm'. 14th Int. Conf. on Harmonics and Quality of Power, Bergamo, 2010, pp. 1–9
21 Samet, H., Farhadi, M.R., Mofrad, M.R.B.: 'Employing artificial neural networks for prediction of electrical arc furnace reactive power to improve compensator performance'. IEEE Int. Energy Conf. and Exhibition (ENERGYCON), Florence, 2012, pp. 249–253

© The Institution of Engineering and Technology 2016

17518695, 2016, 13, Downloaded from https://ietresearch.onlinelibrary.wiley.com/doi/10.1049/iet-gtd.2016.0405, Wiley Online Library on [06/05/2025]. See the Terms and Conditions (https://onlinelibrary.wiley.com/terms-and-conditions) on Wiley Online Library for rules of use; OA articles are governed by the applicable Creative Commons License

22 Samet, H., Golshan, M.E.H.: 'A wide nonlinear analysis of reactive power time series related to electric arc furnaces', *Electr. Power Energy Syst.*, 2012, **36**, (1), pp. 127–134
23 Sadeghian, A.R., Lavers, J.D.: 'Application of radial basis function networks to model electric arc furnace'. Proc. IJCNN Int. Joint Conference on Neural Networks, Washington, 1999, 6, pp. 3996–4001
24 Sharifi, F.J., Jorjani, G.: 'An adaptive system for modelling and simulation of electrical arc furnaces', *Control Eng. Pract.*, 2009, **17**, pp. 1202–1219
25 Chang, G.W., Liu, Y.J., Chen, C.I.: 'Neural-network-based method of modelling electric arc furnace load for power engineering study', *IEEE Trans. Power Syst.*, 2010, **25**, (1), pp. 138–146
26 Sadeghian, A.R., Lavers, J.D.: 'Dynamic reconstruction of nonlinear v–i characteristic in electric arc furnaces using adaptive neuro-fuzzy rule-based networks', *Appl. Soft Comput.*, 2011, **11**, (1), pp. 1448–1456
27 Brusa, E.G.M., Morsut, S.: 'Design and structural optimization of the electric arc furnace through a mechatronic-integrated modeling activity', *IEEE/ASME Trans. Mechatronics*, 2015, **20**, (3), pp. 1099–1107
28 Biro, O., Preis, K., Richter, K.R., *et al.*: 'FEM computation of the forces on the arc of a DC-furnace', *IEEE Trans. Magn.*, 1994, **30**, (5), pp. 3507–3510
29 Akdag, A., Çadirci, I., Nalçaci, E., *et al.*: 'Effects of main transformer replacement on the performance of an electric arc furnace system', *IEEE Trans. Ind. Appl.*, 2000, **36**, (2), pp. 649–658
30 Suh, Y., Park, H., Lee, Y., *et al.*: 'A power conversion system for AC furnace with enhanced arc stability', *IEEE Trans. Ind. Appl.*, 2010, **46**, (6), pp. 2526–2535
31 Samet, H., Masoudipour, I., Parniani, M.: 'New reactive power calculation method for electric arc furnaces', *Measurement*, 2016, **81**, pp. 251–263
32 Morello, S., Dionise, T.J., Mank, T.L.: 'Comprehensive analysis to specify a static var compensator for an electric arc furnace upgrade', *IEEE Trans. Ind. Appl.*, 2015, **51**, (6), pp. 4840–4852

© The Institution of Engineering and Technology 2016

17518695, 2016, 13, Downloaded from https://ietresearch.onlinelibrary.wiley.com/doi/10.1049/iet-gtd.2016.0405, Wiley Online Library on [06/05/2025]. See the Terms and Conditions (https://onlinelibrary.wiley.com/terms-and-conditions) on Wiley Online Library for rules of use; OA articles are governed by the applicable Creative Commons License